Int. J. Heat Mass Transfer. Vol. 24, No. 12, pp. 1971–1981, 1981.
Printed in Great Britain

0017-9310/81/121971-11 $02.00/0

TRANSIENT PHASE-CHANGE AROUND A HORIZONTAL CYLINDER

L. S. YAO and W. CHERNEY
Department of Mechanical and Industrial Engineering, University of Illinois at Urbana-Champaign, Urbana, IL 61801, U.S.A.

(*Received* 19 *May* 1980 *and in revised form* 5 *June* 1981)

Abstract—The integral method is applied to study the effects of the natural convection on the melting of a solid around a hot horizontal cylinder. The results demonstrate that the melting process is affected by the following five dimensionless parameters: subcooling; Rayleigh, Stefan and Prandtl numbers; and the ratio of thermal diffusivities. Their effects are quantitatively assessed. The integral solution shows surprising accuracy when it is compared with the quasi-steady solution when Stefan number is small.

NOMENCLATURE

- a, radius of the hot cylinder;
- B, gap function, equation (3f);
- f, stream function;
- g, gravitation acceleration;
- Pr, Prandtl number;
- q, heat flux along the interface of two phases;
- r, radial coordinate;
- R, contour of the melted region;
- Ra, Rayleigh number;
- Ra_B, $Ra[(2t^{1/2})B]^3$;
- s, stream function parameter, equation (24);
- S_b, subcooling factor, equation (10c);
- S_d, Stefan number, equation (10b);
- T, temperature;
- θ, dimensionless temperature, equations (3a);
- ν, kinematic viscosity;
- α, thermal diffusivity;
- β, thermal expansion coefficient;
- ϕ, time-dependent amplitude of stream function, equation (24);
- ψ, azimuthal coordinate;
- ρ, density.

Superscripts

- $\bar{}$, dimensional quantity;
- $'$, derivative with respect to ψ;
- $\cdot$, derivative with respect to time.

Subscripts

- i, hot cylinder;
- l, melted solid;
- m, melting front;
- s, solid;

Numbers indicate the expansion order.

INTRODUCTION

EFFECTIVE usage of waste heat requires the development of thermal storage systems. Utilization of latent heat during the process of changing phase is one of the viable concepts. Traditionally, convective heat transfer was rarely considered to be important in phase-change processes. Recently, experimental studies [1, 2] have shown that natural convection can have substantial influence on the phase-change process around a heated horizontal cylinder.

Intuitively, one can imagine that heat conduction is the dominant heat transfer mode within a short period after the melting starts. Yao and Chen [3] showed that the magnitude of natural convection increases as the melted region grows and the governing parameter is the Rayleigh number evaluated on the typical distance between the inner hot cylinder and the interface of two phases. Quasi-steady approximation has been used to develop the series solution by treating the effect of natural convection as a perturbation quantity. In their solution, they have assumed that the solid is held at its melting temperature. Thus, no heat transfer inside the solid bed has been considered.

Maintaining the solid bed at its melting temperature without changing its phase is a difficult task in the laboratory. If a few degrees of subcooling in the solid bed exist in the experimental studies of the phase-change problems, the subcooling effect has to be taken into acount in order to accurately interpret experimental data.

In this paper, we study the subcooling effect on the phase-change process around a heated horizontal cylinder. We concentrate on the short-time solution so that the natural convection can be treated as a perturbation quantity. This allows us to separate the azimuthal dependence of the eccentric shape of the melted region and to simplify the analysis.

The detailed mathematical model and the coordinate transformation which immobilizes the interface of the two phases and removes the singularity at the beginning of the melting process are given in the next section. The regular perturbation solution is developed in the third section. The corresponding approximate integral formulation and the numerical procedure to integrate the final ordinary differential equations are described in the fourth section. In the fifth section, the numerical results are presented and discussed.

MATHEMATICAL FORMULATION

The physical model considered is an infinitely long circular cylinder of radius a horizontally embedded in an infinite solid, Fig. 1. Initially, T_s is held below T_m. The position of the melting front is denoted by $R(\psi, \bar{t})$. Conduction is dominant at the beginning of the melting process. As the melted region increases, the effect of natural convection gradually appears, and disturbs the temperature distribution. The melted region forms an eccentric annulus. The importance of the natural convection depends on the Rayleigh number which increases as the third power of the gap of the melted region. Hence, the convection heat transfer eventually becomes the dominant mode.

Melted solid

In this paper we consider the short-time solution which is valid before the convection becomes the dominant mode. The formulation is, however, valid for general phase-change problems in cylindrical coordinates. The variation of density through phase change is not considered; however, the buoyancy forces induced by the density stratification is included. This is known as the Boussinesq approximation.

The governing equations for the region of melted solid in cylindrical polar coordinates are:

$$\frac{\partial(\bar{r}\bar{u})}{\partial \bar{r}} + \frac{\partial \bar{v}}{\partial \psi} = 0 \tag{1a}$$

$$\frac{\partial \bar{u}}{\partial \bar{t}} + \bar{u}\frac{\partial \bar{u}}{\partial \bar{r}} + \frac{\bar{v}}{\bar{r}}\frac{\partial \bar{u}}{\partial \psi} - \frac{\bar{v}^2}{\bar{r}} = \frac{-1}{\rho_l}\frac{\partial \bar{p}}{\partial \bar{r}} - \beta g(T - T_m)\cos\psi - \frac{\nu}{\bar{r}}\frac{\partial}{\partial \psi}\left[\frac{\partial \bar{v}}{\partial \bar{r}} + \frac{\bar{v}}{\bar{r}} - \frac{1}{\bar{r}}\frac{\partial \bar{u}}{\partial \psi}\right], \tag{1b}$$

$$\frac{\partial \bar{v}}{\partial \bar{t}} + \bar{u}\frac{\partial \bar{v}}{\partial \bar{r}} + \frac{\bar{v}}{\bar{r}}\frac{\partial \bar{v}}{\partial \psi} + \frac{\bar{u}\bar{v}}{\bar{r}} = \frac{-1}{\rho_l \bar{r}}\frac{\partial \bar{p}}{\partial \psi} + \beta g(T - T_m)\sin\psi + \nu\frac{\partial}{\partial \bar{r}}\left[\frac{\partial \bar{v}}{\partial \bar{r}} + \frac{\bar{v}}{\bar{r}} - \frac{1}{\bar{r}}\frac{\partial \bar{u}}{\partial \psi}\right], \tag{1c}$$

$$\frac{\partial T}{\partial \bar{t}} + \bar{u}\frac{\partial T}{\partial \bar{r}} + \frac{\bar{v}}{\bar{r}}\frac{\partial T}{\partial \psi} = \alpha_l\left[\frac{\partial^2 T}{\partial \bar{r}^2} + \frac{1}{\bar{r}}\frac{\partial T}{\partial \bar{r}} + \frac{1}{\bar{r}^2}\frac{\partial^2 T}{\partial \psi^2}\right]. \tag{1d}$$

The boundary conditions associated with equation (1) are:

$\bar{t} \geq 0$,

$$T = T_i \quad \text{and} \quad \bar{u} = \bar{v} = 0 \quad \text{at } \bar{r} = a; \tag{2a}$$

$$T = T_m \quad \text{and} \quad \bar{u} = \bar{v} = 0 \quad \text{at } \bar{r} = R(\psi, t). \tag{2b}$$

The following dimensionless variables are introduced to non-dimensionalize equations (1). They are:

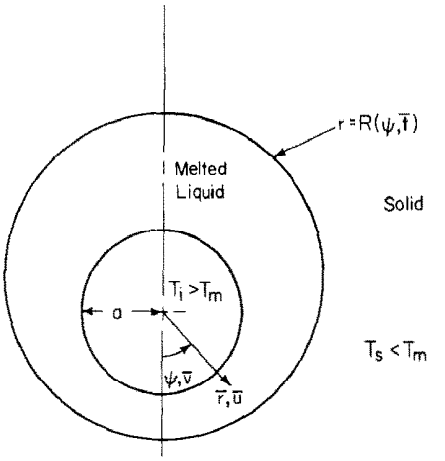

FIG. 1. Physical model and coordinates.

$$u = \bar{u}/(\alpha_l/a), \quad v = \bar{v}/(\alpha_l/a), \quad \text{(velocities)} \tag{3a}$$

$$p = \bar{p}/(\rho_l \alpha_l^2/a^2), \quad \text{(pressure)} \tag{3b}$$

$$\theta_l = (T - T_m)/(T_i - T_m), \quad \text{(temperature)} \tag{3c}$$

$$t = \bar{t}/(a^2/\alpha_l), \quad \text{(time)} \tag{3d}$$

$$r = (\bar{r} - a)/[a(2t)^{1/2}B(\psi, t)], \quad \text{(radial coordinate)} \tag{3e}$$

$$B(\psi, t) = [R(\psi, \bar{t}) - a]/[a(2t)^{1/2}], \quad \text{(melting front)} \tag{3f}$$

$$Ra = \beta g(T_i - T_m)a^3/(\alpha_l \nu), \quad \text{(Rayleigh no.)} \tag{3g}$$

$$Pr = \alpha_l/\nu, \quad \text{(Prandtl no.)} \tag{3h}$$

$$\alpha_{sl} = \alpha_s/\alpha_l, \quad \text{(ratio of thermal diffusivities).} \tag{3i}$$

Substitution of equations (3) into equations (1) gives:

$$\partial/\partial r_l\{[r_l + 1/((2t)^{1/2}B)]u\} + \partial v/\partial \psi = (r_l B'/B)\partial v/\partial r_l; \tag{4a}$$

$$\frac{1}{Pr}\left\{\frac{\partial u}{\partial t} + \frac{1}{(2t)^{1/2}B}\left[u - \frac{r_l}{(2t)^{1/2}}(2t\dot{B} + B) - \frac{r_l B' v}{B[r_l + 1/((2t)^{1/2}B)]}\right]\frac{\partial u}{\partial r_l} + \frac{v}{(2t)^{1/2}B[1 + 1/((2t)^{1/2}B)]}\left(\frac{\partial u}{\partial \psi} - v\right)\right\}$$
$$= -\frac{1}{(2t)^{1/2}B}\frac{\partial p}{\partial r_l} - Ra\,\theta\cos\psi - \frac{1}{(2t)B^2[r_l + 1/((2t)B^{1/2}B)]}\frac{\partial}{\partial \psi} \times \left[\frac{\partial v}{\partial r_l} + \frac{1}{[r_l + 1/((2t)^{1/2}B)]} \times \left(v - \frac{\partial u}{\partial \psi} + \frac{r_l B'}{B}\frac{\partial u}{\partial r_l}\right)\right]$$

$$+\frac{rB'}{(2t)B^3[r_l+1/((2t)^{1/2}B)]}\frac{\partial}{\partial r_l}\times\left[\frac{\partial v}{\partial r_l}+\frac{1}{[r_l+1/((2t)^{1/2}B)]}\times\left(v-\frac{\partial u}{\partial\psi}+\frac{r_lB'}{B}\frac{\partial u}{\partial r_l}\right)\right]; \quad (4b)$$

$$\frac{1}{Pr}\left\{\frac{\partial v}{\partial t}+\frac{1}{(2t)^{1/2}B}\left[u-\frac{r_l}{(2t)^{1/2}}(2t\dot{B}+B)-\frac{r_lB'v}{B[r_l+1/((2t)^{1/2})B]}\right]\frac{\partial v}{\partial r_l}+\frac{v}{[(2t)^{1/2}B][r_l+1/((2t)^{1/2}B)]}\left[\frac{\partial v}{\partial\psi}+u\right]\right\}$$
$$=\frac{-1}{[(2t)^{1/2}B][r_l+1/((2t)^{1/2}B)]}\frac{\partial p}{\partial\psi}+Ra\,\theta\sin\psi+\frac{1}{(2t)B^2}\frac{\partial}{\partial r_l}\times\left[\frac{\partial v}{\partial r_l}+\frac{1}{r_l+[1/((2t)^{1/2}B)]}\times\left(v-\frac{\partial u}{\partial\psi}+\frac{r_lB'}{B}\frac{\partial u}{\partial r}\right)\right]; \quad (4c)$$

$$\frac{\partial\theta_l}{\partial t}+\frac{1}{(2t)^{1/2}B}\left[u-\frac{r_l}{(2t)^{1/2}}(2t\dot{B}+B)-\frac{r_lB'v}{(2t)^{1/2}B[r_l+1/((2t)^{1/2}B)]}\right]\frac{\partial\theta_l}{\partial r_l}+\frac{v}{(2t)^{1/2}B[r_l+1/((2t)^{1/2}B)]}\frac{\partial\theta_l}{\partial\psi}$$
$$=\frac{1}{2tB^2}\left\{\frac{\partial^2\theta_l}{\partial r_l^2}+\frac{1}{[r_l+1/((2t)^{1/2}B)]}\frac{\partial\theta_l}{\partial r_l}+\frac{1}{[r_l+1/((2t)^{1/2}B)]^2}\left(\frac{\partial}{\partial\psi}-r_l(B'/B)\frac{\partial}{\partial r_l}\right)^2\theta_l\right\}. \quad (4d)$$

The boundary conditions (2) become:

$t\geq 0$,

$$\theta_l=1 \quad \text{and} \quad u=v=0 \quad \text{at } r_l=0, \quad (5a)$$

$$\theta_l=0 \quad \text{and} \quad u=v=0 \quad \text{at } r_l=1. \quad (5b)$$

The choice of the dimensionless radial coordinate has two purposes: (1) to transform the melted region into a unit circle and (2) to remove the singularity at $t=0$. A similar transformation has been used to study the natural convection in the melted region in the neighborhood of a heated vertical cylinder [4] and to study the melting of a subcooled solid around a heated circular cylinder due to the heat conduction [5]. It is worth pointing out the convection effects induced by the moving boundary is included in the formulation.

The singularity of the equations for the phase-change problem at $t=0$ has been recognized for a long time. Neumann in 1912 and Stefan in 1891 [6] solved the phase-change problem of a semi-infinite solid in terms of a similarity variable, the ratio of the distance from the interface at zero time to the square root of time. In other words, the melting front propagates proportional to $t^{1/2}$.

For a cylindrical geometry, the gap between the inner cylinder and the interface is small compared with the radius of the inner cylinder within a short while after the melting starts. Thus, the effect of transverse curvature is negligible. Therefore, Neumann's solution is also applicable to the cylindrical geometry at the beginning of the melting. This is why the radial coordinate is scaled by the square root of time [see equation (3f)].

Solid bed

The dimensionless unsteady conduction equation for the solid bed is

$$(2t)\frac{\partial\theta_s}{\partial t}-(2t\dot{B}+r_s+B)\frac{\partial\theta_s}{\partial r_s}=\alpha_{sl}\left[\frac{\partial^2}{\partial r_s^2}+\frac{(2t)^{1/2}}{(2t)^{1/2}B+r_s+1}\frac{\partial}{\partial r_s}+\frac{2t}{[(2t)^{1/2}B+r_s+1]^2}\left(\frac{\partial}{\partial\psi}-B'\frac{\partial}{\partial r_s}\right)^2\right]\theta_s \quad (6)$$

where α_{sl} is the ratio of thermal diffusivities of the solid to the liquid.

The associated dimensionless variables are:

$$\theta_s=(T-T_m)/(T_m-T_s), \quad \text{(temperature)} \quad (7a)$$

$$r_s=(\bar{r}-R(\psi,t)/[a(2t)^{1/2}]. \quad \text{(radial coordinate)} \quad (7b)$$

Scaling the radial coordinate of the solid bed by $(2t)^{1/2}$ has the advantage that it reduces the ever increasing thermal penetration depth in the solid; also, it removes the singularity at $t=0$.

The required boundary conditions are

$$t<0, \quad \theta_s=-1, \quad \text{(no melted region)} \quad (8a)$$

$$t\geq 0, \quad \theta_s=0 \quad \text{at } r_s=0, \quad (8b)$$

$$\theta_s\to -1 \quad \text{as } r_s\to\infty. \quad (8c)$$

Interface

The equation governing the location of the melting front can be obtained by taking an energy balance along the interface of the melted region and the solid bed. In the dimensionless form, it is:

$$(-1/\bar{B})\{[1+(r\bar{B}'^2)/[\bar{B}(r_l+1/\bar{B})^2]\}\frac{\partial\theta}{\partial r_l}$$

$$- [\bar{B}'/(r_l + 1/\bar{B})^2]\frac{\partial \theta_l}{\partial \psi}\Big\}_{r_l=1}$$
$$+ S_b\Big\{[1 + \bar{B}'^2/(r_l + \bar{B} + 1)^2]\frac{\partial \theta_s}{\partial r_s}$$
$$- [\bar{B}'/(r_l + \bar{B} + 1)^2]\frac{\partial \theta_s}{\partial \psi}\Big\}_{r_s=0} = \frac{1}{s_d}\frac{\partial \bar{B}}{\partial t} \quad (9)$$

where

$$\bar{B} = (2t)^{1/2}B, \quad (10a)$$

$$S_d = (\rho_s C_s/\rho_l C_l)[C_l(T_1 - T_m)/L],$$
(Stefan Number) (10b)

$$S_b = k_s(T_m - T_s)/[k_l(T_1 - T_m)],$$
(subcooling factor). (10c)

Due to the complexity of the governing equations, it is unlikely to solve them in a closed form. Numerical method may be the only choice if one is interested in the long-time solution. Partial immobilization of the penetration depth and transformation of the asymmetric melted region into a circle can substantially simplify the numerical computation.

In this paper, we concentrate on the short-time solution where the natural convection can be treated as a perturbed effect. The series of the regular perturbation solution is developed in the next section. The approximate integral solutions are then described in the fourth section.

Analysis

Rayleigh number defined in equation (3g) is based on the radius of the inner cylinder. Equations (4b, c) can be rearranged to show that the buoyancy forces are proportional to $Ra_B = [(2t)^{1/2}B]^3 Ra$. This shows that the importance of the natural convection rapidly increases with the size of the melted region. However, at the beginning of the melting process, most energy is transferred by conduction. Within a short period after the melting starts, the effect of natural convection can be treated as the perturbed quantities. The short-time solution is obtained by the regular perturbation method in the paper.

The convenient expansion parameter is Ra. However, the solution is not limited by the value of Ra but is only valid for small Ra_B, i.e. short-time solution.

Melted solid

For the melted region, the dependent variables can be expanded as

$$\theta_l = \theta_{l,0}(r_l, t) + Ra\cos\psi\theta_{l,1}(r_l, t) + \dots \quad (11a)$$
$$f = Ra\sin\psi f_1(r_l, t) + \dots \quad (11b)$$
$$p = Ra\sin\psi p_{l,1}(r_l, t) + \dots \quad (11c)$$
$$B = B_0(t) + Ra\cos\psi B_1(t) + \dots \quad (11d)$$

where f is the stream function and is related to the velocities as:

$$\left.\begin{aligned} u &= \frac{-1}{1 + (2t)^{1/2}Br_l}\left[\frac{\partial f}{\partial \psi} - \frac{B'}{B}\left(r_l\frac{\partial f}{\partial r_l}\right)\right] \\ \text{and} \\ v &= \frac{1}{(2t)^{1/2}B}\frac{\partial f}{\partial r_l}. \end{aligned}\right\} \quad (12)$$

After elimination of p between equations (4b, c) and replacing u and v by f, then substitution of equations (11) into equations (4) and collection of equal order Ra terms gives:

$$(Ra^0): (2t)B_0^2\frac{\partial \theta_{l,0}}{\partial t} - r_l B_0^2\left[1 + (2t)\frac{\dot{B}_0}{B_0}\right]\frac{\partial \theta_{l,0}}{\partial r_l}$$
$$= \frac{\partial^2 \theta_{l,0}}{\partial r_l^2} + \frac{1}{r_l + 1/[(2t)^{1/2}B_0]}\frac{\partial \theta_{l,0}}{\partial r_l}; \quad (13)$$

$$(Ra): (2t)B_0^2\frac{\partial \theta_{l,1}}{\partial t} - r_l B_0[2t\dot{B}_0 + B_0]\frac{\partial \theta_{l,1}}{\partial r_l}$$
$$- \frac{(2t)^{1/2}B_0 f_1}{r_l + 1/[(2t)^{1/2}B_0]} + 2tr_l$$
$$\times (\dot{B}_0 B_1 - B_0\dot{B}_1)\frac{\partial \theta_{l,0}}{\partial r_l}$$
$$= \nabla_1^2\theta_{l,1} - 2\frac{B_1}{B_2}\frac{\partial^2 \theta_{l,0}}{\partial r_l^2} - \frac{B_1}{B_2}$$
$$\times \frac{1}{r_l + 1/[(2t)^{1/2}B_0]}$$
$$\times 1 - \frac{1 - 1/[(2t)^{1/2}B_0]}{r_l + 1/[(2t)^{1/2}B_0}\frac{\partial \theta_{l,0}}{\partial r_l}; \quad (14a)$$

$$\left[\frac{2tB_0^2}{Pr}\frac{\partial}{\partial t} - \nabla_1^2\right]\cdot\nabla_1^2 f_1 = (2tB_0^2)\frac{\partial \theta_{l,0}}{\partial r_l} + \frac{1}{Pr}$$
$$\times \frac{B_0(2t\dot{B}_0 + B_0)}{r_l + 1/[(2t)^{1/2}B_0]}r_l\left[r_l + \frac{1}{(2t)^{1/2}B_0}\right]\frac{\partial^3 f_1}{\partial r_l^3}$$
$$+ 2r_l + \frac{1}{(2t)^{1/2}B_0}\frac{\partial^2 f_1}{\partial r_l^2} - \frac{r_l}{r_l + 1/[(2t)^{1/2}B_0]}\frac{\partial f_1}{\partial r_l}$$
$$+ \frac{f_1}{r_l + 1/[(2t)^{1/2}B_0]}; \quad (14b)$$

where

$$\nabla_1^2 = \frac{\partial^2}{\partial r_l^2} + \frac{1}{r_l + 1/[(2t)^{1/2}B_0]}\frac{\partial}{\partial r_l}$$
$$- \frac{1}{[r_l + 1/((2t)^{1/2}B_0)]^2}. \quad (14c)$$

Equation (13) shows that the leading term of the energy transfer in the melted region is the conduction mode. The second term of equation (13) represents the effect induced by the moving boundary which is similar to the convection effect along the radial direction. The terms on the right-hand side of equation (13) represent heat diffusion.

Similar interpretation can be given to equation (14a). The term multiplied by f_1 is the contribution due to the natural convection equation (14b) which describes the fluid flow due to buoyancy forces.

Solid bed

The temperature distribution in the solid bed can be expanded as:

$$\theta_s = \theta_{s,0}(r_s, t) + Ra \cos\psi\theta_{s,1}(r_s, t) + \ldots . \quad (14d)$$

The equations governing θ_s's can be obtained by substituting equation (14d) into equation (6). They are

$$(Ra^0): (2t)\frac{\partial\theta_{s,0}}{\partial t} - [r_s + B_0 + 2t\dot{B}_0]\frac{\partial\theta_{s,0}}{\partial r_s} = \alpha_{sl}\frac{\partial^2\theta_{s,0}}{\partial r_s^2} + \frac{1}{r_s + B_0 + 1/(2t)^{1/2}}\frac{\partial\theta_{s,0}}{\partial r_s}; \quad (15a)$$

$$(Ra): (2t)\frac{\partial_{s,1}}{\partial t} - (r_s + B_0 + 2t\dot{B}_0)\frac{\partial\theta_{s,1}}{\partial r_s} - (2t\dot{B}_1 + B_1)\frac{\partial\theta_{s,0}}{\partial r_s} = \alpha_{sl}\nabla_2^2\theta_{s,1}; \quad (15b)$$

where

$$\nabla_2^2 = \frac{\partial^2}{\partial r_s^2} + \frac{1}{r_s + B_0 + 1/(2t)^{1/2}}\frac{\partial}{\partial r_s} - \frac{1}{[r_s + B_0 + 1/(2t)^{1/2}]^2}. \quad (15c)$$

Interface

The equations governing the location of the melting front are:

$$(Ra^0): (2t)\dot{B}_0 + B_0 = S_d S_b \left.\frac{\partial\theta_{s,0}}{\partial r_s}\right|_{r_s=0} - \frac{1}{B_0}\left.\frac{\partial\theta_{l,0}}{\partial r_l}\right|_{r=1}; \quad (16a)$$

$$(Ra): (2t)\dot{B}_1 + B_1 = S_d S_b \left.\frac{\partial\theta_{s,1}}{\partial r_s}\right|_{r_s=0} - \frac{1}{B_0}\frac{\partial\theta_{l,1}}{\partial r_l} - \frac{B_1}{B_0}\left.\frac{\partial\theta_{l,0}}{\partial r_l}\right|_{r_l=1}. \quad (16b)$$

The associated boundary conditions can be obtained straightforwardly by substitution of the expansion series into equations (5) and (8) and collection of equal-order terms of Ra. They are listed below:

(i) Melted solid:

$$\text{At } r_l = 0 \quad \theta_{l,0} = 1, \quad \theta_{l,1} = f_1 = f_{1,r_l} = 0, \quad (17a)$$

$$\text{At } r_l = 1 \quad \theta_{l,0} = \theta_{l,1} = f_1 = f_{1,r_l} = 0. \quad (17b)$$

(ii) Solid bed:

$$\text{At } r_s = 0 \quad \theta_{s,0} = \theta_{s,1} = 0, \quad (18a)$$

$$\text{At } r_s \to \infty \quad \theta_{s,0} \to -1, \quad \theta_{s,1} \to 0. \quad (18b)$$

INTEGRAL FORMULATION

Solid bed

The temperature distribution in the solid bed is assumed as a 2nd-order polynomial. The parameter that governs the heat transfer rate is the heat penetration depth, δ. For the short-time solution, the penetration depth can also be expanded as

$$\delta = \delta_0(t) + Ra\cos\psi\delta_1(t) + \ldots . \quad (19)$$

The assumed temperature distributions which satisfy the boundary conditions (18) are

$$\theta_{s,0} = -2(r_s/\delta_0) + (r_s/\delta_0)^2, \quad (20a)$$

$$\theta_{s,1} = 2(\delta_1/\delta_0)[(r_s/\delta_0) - (r_s/\delta_0)^2]. \quad (20b)$$

The governing equations for δ_0 and δ_1 can be obtained by substituting equations (20) into equations (15) and then integrating them from $r_s = 0$ to $r_s = \delta$. They are

$$(\delta_0 t)\dot{\delta}_0 + (\delta_0^2/2) + (3/2)\delta_0(2t\dot{B}_0 + B_0) = \alpha_{sl}\left\{6 + [3/\delta_0(2t)^{1/2}][1 + (\delta_0 + B_0)] \times (2t)^{1/2}\ln\frac{1 + B_0(2t)^{1/2}}{1 + (\delta_0 + B_0)(2t)^{1/2}}\right\} \quad (21a)$$

and

$$\frac{2t}{3}\dot{\delta}_1 + \frac{1}{3} + \frac{2S_bS_d}{\delta_0^2} + \alpha_{sl}\frac{4}{\delta_0^2}\delta_1 = S_d\left[\frac{q_0B_1}{B_0^2} - \frac{q_1}{B_0}\right]. \quad (21b)$$

Melted solid

The temperature distribution in the region of melted solid is expressed in terms of the heat flux, q, along the interface of two phases. For the short-time solution, q can be expanded as

$$q = q_0(t) + Ra\cos\psi q_1(t) + \ldots . \quad (22)$$

The assumed temperature profiles which satisfy the boundary conditions are

$$\theta_{l,0} = 1 - (2 - q_0)r_l + (1 - q_0)r_l^2 \quad (23a)$$

and

$$\theta_{l,1} = q_1(r_l - r_l^2). \quad (23b)$$

The stream function f_1 is assumed as

$$f_1 = \phi(t)[(r_l^4 - 2r_l^3 + r_l^2) - s(r_l^5 - 2r_l^4 + r_l^3)] \quad (24)$$

which satisfies the no-slip condition on the solid walls. The method of selecting s will be discussed in the Results and Discussion section.

Substitution of equation (24) into equations (13) and (14) and then integration from $r_l = 0$ to $r_l = 1$ yield.

$$(2tB_0^2)\dot{q}_0 + (2 + q_0)(B_0^2 + 2tB_0\dot{B}_0) = 24(1 - q_0) - 6(2 - q_0) + (2 - 2q_0)/[(2t)^{1/2}B_0] \times \ln[1 + (2t)^{1/2}B_0], \quad (25)$$

$$\phi(t) = C^2/[24 - (4C^2/1 + C) + 2/PrB_0$$

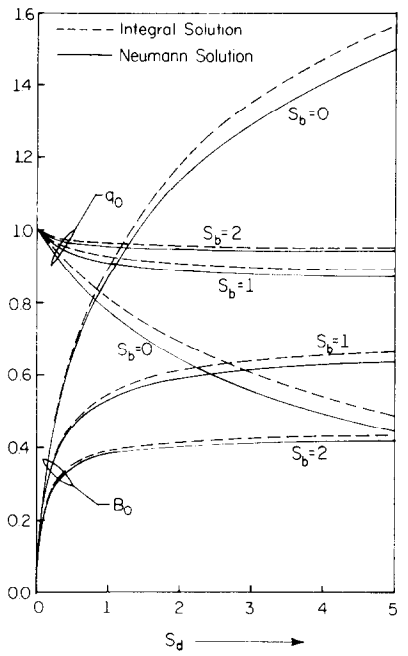

FIG. 2. Comparison of the integral solution with Neumann solution at $t = 0$ and $\alpha_{sl} = 1$.

$$\times(2t\dot{B}_0 + B_0)] - S[12 + (4C/1 + C) + (2/Pr)B_0(2t\dot{B}_0 + B_0)], \quad (26)$$

and

$$C^2\dot{q}_1 + (12 + B_0^2 + 2tB_0\dot{B}_0)q_1 = (2t)^{1/2}(2 + q_0)(\dot{B}_0B_1 - B_0\dot{B}_1)/B_0 + 6\phi(C_2 - SC_3) - B_1/B_0)\{36(1 - q_0) - 6\ln(1 + C) \times [(2 - q_0) + (2 - 2q_0)/C]\} \quad (27a)$$

where

$$C_2 = (C/15)(1 - q_0) - [C(2 - q_0) + (2 - 2q_0)] \times [(1/12 - 1/3C - 3/2C^2 - 1/C^3) + (1/C^2 + 2/C^3 + 1/C^4)\ln(1 + C)], \quad (27b)$$

$$C_3 = (C/30)(1 - q_0) - [C(2 - q_0) + (2 + 2q_0)] \times [(1/30 - 1/12C + 1/3C^2 + 3/2C^3 + 1/C^4) - (1/C^3 + 2/C^4 + 1/C^5)\ln(1 + C)], \quad (27c)$$

$$C = 2t \times B_0. \quad (27d)$$

Interface

Substitution of equations (20) and (24) into equations (16) and taking the appropriate limit result

$$(2t)\dot{B}_0 + B_0 = S_d[q_0/B_0 - 2S_b/\delta_0] \quad (28a)$$

and

$$(2t)\dot{B}_1 + B_1 = S_d[q_1/B_0 - q_0B_1/B_0^2 + 2S_b\delta_1/\delta_0^2]. \quad (28b)$$

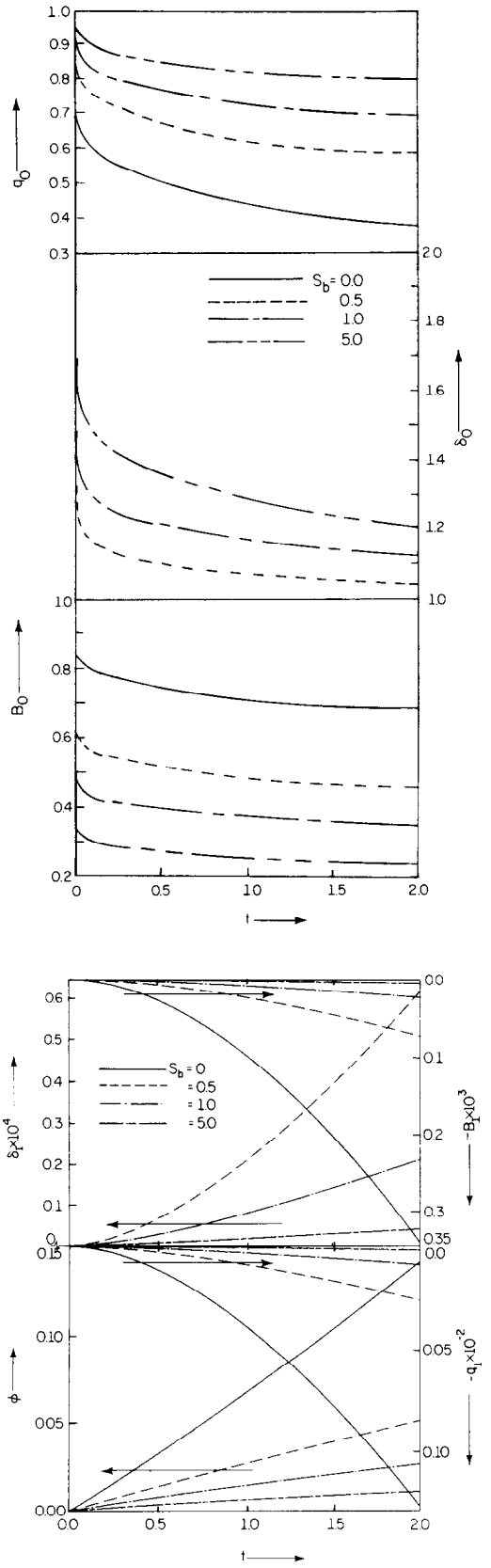

FIG. 3.(a) Subcooling effects (zeroth-order solutions at $S_d = 1$, $\alpha_{sl} = 1$); (b) subcooling effects (1st-order solutions at $Pr = 1$, $S_d = 1$, $\alpha_{sl} = 1$).

Numerical integration and initial conditions

Radial-coordinate transformations (3e, f) and (17b) remove the singularity at $t = 0$. The required initial conditions to start integrating equations (21), (22), (25), (26b), and (28a, b) can be obtained from these equations by taking the limit that $t \to 0$. They are

$$O(Ra^0) = \begin{cases} q_0(0) = (12 - 2B_0^2)/(12 + B_0^2) & (29a) \\ \delta_0(0) = (2.25B_0^2 + 6\alpha_{sl})^{1/2} - 1.5B_0 & (29b) \\ B_0(0) = S_d\{(12 - 2B_0^2)/(12B_0 + B_0^3) \\ \qquad - 2S_b/[2.25B_0^2 + 6\alpha_{sl})^{1/2} \\ \qquad - 1.5B_0] & (29c) \end{cases}$$

and

$$O(Ra) = \begin{cases} \phi = 0 & (30a) \\ q_1 = -12B_1(1 - q_0)/(12B_0 + B_0^3) & (30b) \\ \delta_1 = \delta_0^2 B_1/[\delta_0 B_0 - \delta_0^2/3 - 4\alpha_{sl}(1 + \delta_0)] & (30c) \\ B_1 = S_d(q_1/B_0 + 2S_b\delta_1/\delta_0^2)/(1 + S_d q_0/B_0^2). & (30d) \end{cases}$$

Equations (29) are non-linear. The value of $q_0(0)$ and $\delta_0(0)$ can be determined after obtaining B_0 from equation (29c) by iterations. The procedure is straightforward and obvious; therefore, we do not describe it here. It is worth pointing out that equations (29) are the approximate integral solution of the Neumann problem. The Neumann solution in the transformed coordinates are listed below in order to determine the accuracy of the integral solution.

The Neumann solution is

$$B_0 = S_d(2/\pi)^{1/2}\{e^{-B_0^2/2}/\mathrm{erf}(B_0/2^{1/2}) - [S_b/(\alpha_{sl}^{1/2})e^{-B_0^2/(2\alpha_{sl})}]/[1 - \mathrm{erf}(B_0/(2\alpha_{sl})^{1/2})2]\} \quad (31a)$$

and

$$q_0 = (B_0/\pi^{1/2})e^{-B_0^2/2}/\mathrm{erf}(B_0/2^{1/2}) \quad (31b)$$

where erf stands for the error function.

Equations (29a, c) are compared with equations (31) for $\alpha_{sl} = 1$ and various values of S_d and S_b. The results are given in Fig. 2.

The initial values of B_0, the zeroth-order gap function, are plotted as the function of the Stefan number, S_d, for different degrees of subcooling in Fig. 3a. The error of the integral solution at $t = 0$ is bounded by 5% for S_d up to 10, and is smaller for a more subcooled solid bed. The difference of the integral solution and Neumann solution is negligible for $S_d < 0.5$. Figure 3b shows the comparison of q_0's predicted by the integral and Neumann solutions. The maximum error of q_0 by the integral method is bounded by 10% and decreases drastically when the subcooling increases.

The solutions of equations (30), initial conditions for the 1st-order equations, are trivial, i.e.

$$q_1 = B_1 = \delta_1 = 0. \quad (31)$$

The zeroth-order solution, δ_0, q_0, and B_0 are obtained by numerical integration of equations (21), (25) and (28a). The implicit difference scheme is used, the coefficients of the non-linear terms are evaluated by their latest values in iterations. No more than three iterations are needed to obtain the convergent results for most time steps. Several time steps have been tried. The error is bounded by 0.001 for $\Delta t = 0.01$. All results presented in the paper are calculated by taking $\Delta t = 0.01$.

The magnitude of natural convection ϕ can be determined from equation (26) as soon as B_0 is determined. The effect of natural convection on heat transfer, δ_1, q_1, and B_1 can be obtained by a similar numerical procedure. However, $\dot{B}_0$ and $\dot{B}_1$ are eliminated between equations (21b), (26b) and (28) in order to remove the singularity at $t = 0$. Then the implicit method is used to integrate equations (28b), (32) and (33) to obtain B_1, δ_1, and q_1 numerically. After several time steps have been tried, we find that the time step, $\Delta t = 0.01$, selected for the zeroth-order solution is sufficient for the 1st-order solutions.

RESULTS AND DISCUSSION

There are five dimensionless parameters which affect the melting of solid around a hot horizontal cylinder: S_b, the subcooling factor; S_d, the Stefan number; α_{sl}, the ratio of thermal diffusivities of two phases; and Pr and Ra, the Prandtl and Rayleigh numbers, respectively.

Ra is defined in equation (3g) and is used as the expansion parameter is developing the perturbation solution. The perturbation solution, is however, not restricted by the value of Ra but would only be applied for small Ra_B. Since the value of Ra can be changed only by varying $T_1 - T_m$ when the material of the solid bed is selected, Ra can be interpreted as the dimensionless overheating degrees of the hot cylinder. Within a short period of time after the phase change starts, heat conduction is the dominant mode in melting the solid. The effects of free convection is proportional to Ra_B. No existing experimental data have the required accuracy to compare with the results of the analysis within the short while after the melting starts. Therefore, the validity of the perturbation solution can only be determined by comparing the perturbation solution with the exact solution, say a numerical solution, which is, unfortunately, unavailable at present. However, the upper limit that the perturbation solution is valid can be roughly estimated by ruling out the possibility of the resolidification along $\psi = 0°$ which violates the second thermodynamic law. Applying the above criterion, the upper limit is found to be $Ra_B \simeq 2000$.

The effects of S_b, S_d, α_{sl}, and Pr are demonstrated below. $S_b = 1$, $S_d = 1$, $\alpha_{sl} = 1$, and $Pr = 1$ are selected

as the standard case for the convenience of comparison. The value of S is set equal to zero for the data presented in Figs. 3–6.

The subcooling factor, S_b, is defined in equation (10b). Its physical meaning can be interpreted as the ratio of heat conduction inside the solid to that inside the melted region. The zeroth-order solutions (heat conduction) are given in Fig. 3a for $S_b = 0, 0.5, 1$ and 2, respectively.

The term q_0, defined in equation (23a), is the heat flux out of the melted region. Its value drops as the melted region grows. This is because the conduction distance between the surface of the hot cylinder and the melting front gradually increases as the melted region grows. As expected, subcooling increases the surface heat flux. The extent of its influence is more marked at lower degrees of subcooling.

The zeroth-order location of the melting front is represented by $(2t)^{1/2}B_0$. The melting front continuously moves away from the hot cylinder as more solid melts. The scaling $(2t)^{1/2}$ removes most of the growth of the melting front with time; therefore, it allows adoption of a larger time step in numerical integration of equations (28). The melting front moves slower at higher degrees of subcooling as more thermal energy is consumed in warming the subcooled solid bed.

The penetration depth of heat conduction inside the solid is evaluated by $(2t)^{1/2}\delta_0$. The reason for scaling $(2t)^{1/2}$ is similar to that of the melting front. The value of δ_0 is smaller at lower degrees of subcooling. This is because the conduction is suppressed by the convection which is induced by the moving melting front. $\delta_0 = 0$ when there is no subcooling.

The 1st-order solution (free convection) is given in Fig. 3b. The magnitude of the free convection is given by ϕ. Subcooling suppresses the free convection since there is less melted solid at higher degrees of subcooling. The values of q_1, and δ_1 vary proportionally to ϕ.

The Stefan number, S_d, is defined in equation (10b). It represents the ratio of the thermal capacity of the melted solid to the latent heat. It is expected that there is a slower melting at smaller values of S_d. In Fig. 4a, B_0, q_0, and δ_0 are plotted for $S_d = 0.1$, 1, and 5, respectively. With decreasing S_d values, one obtains a smaller B_0. The variation of B_0 is more profound at lower range S_d's. Since it requires a larger amount of thermal energy to melt the solid at a smaller S_d, q_0 decreases as S_d increases. Also δ_0 decreases as S_d decreases due to the fact that the heat conduction penetrates farther for a slower moving melting front. The effects of the free convection are proportional to the melted solid, ϕ, q_1, δ_1, and B_1 increase with S_d as shown in Fig. 4b.

The ratio of thermal diffusivities of two phases, α_{sl}, affects the speed of conducting heat in two different phases. Its effect on q_0, B_0, and δ_0 are given in Fig. 5a for $\alpha_{sl} = 0.5, 1$ and 5, respectively. A larger α_{sl} implies a faster heat conduction in solid. Consequently, more

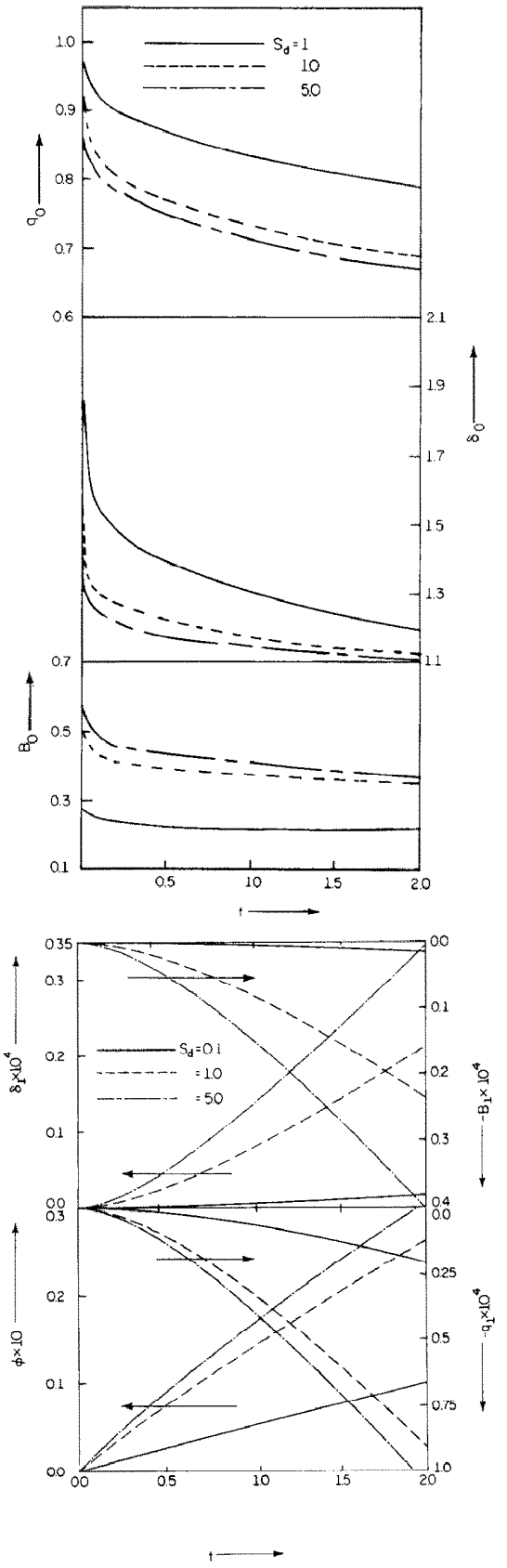

FIG. 4. (a) Stefan number effects (zeroth-order solution at $S_b = 1, \alpha_{sl} = 1$); (b) Stefan number effects (1st-order solution at $Pr = 1$, $S_b = 1$, $S_d = 1$).

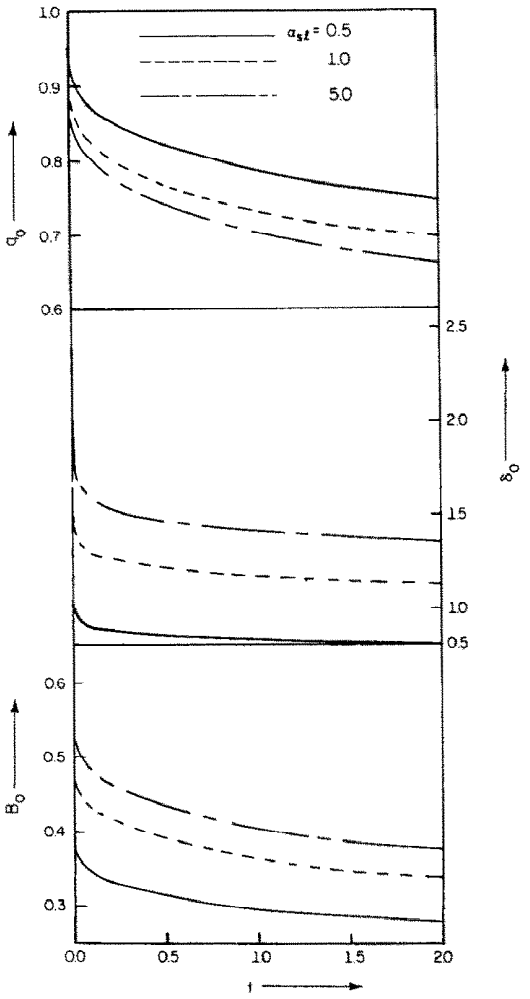

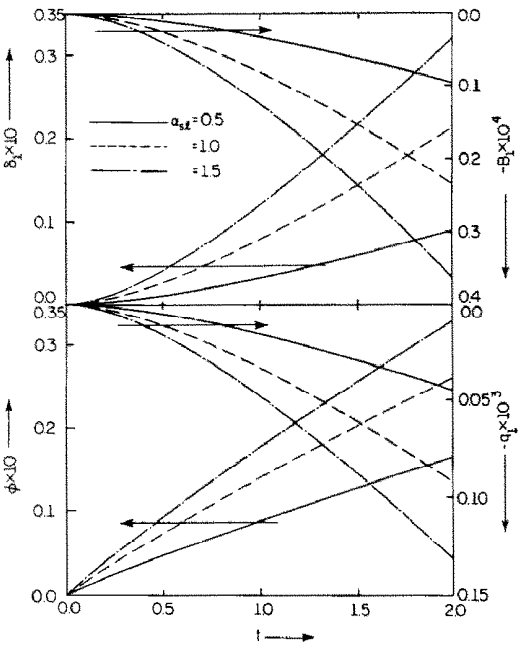

FIG. 5. (a) Effects of thermal diffusivity (zeroth-order solution at $Pr = 1$, $S_b = 1$, $S_d = 1$); (b) effects of thermal diffusivity ($Pr = 1$, $S_b = 1$, $S_d = 1$, $\alpha_{sl} = 1$).

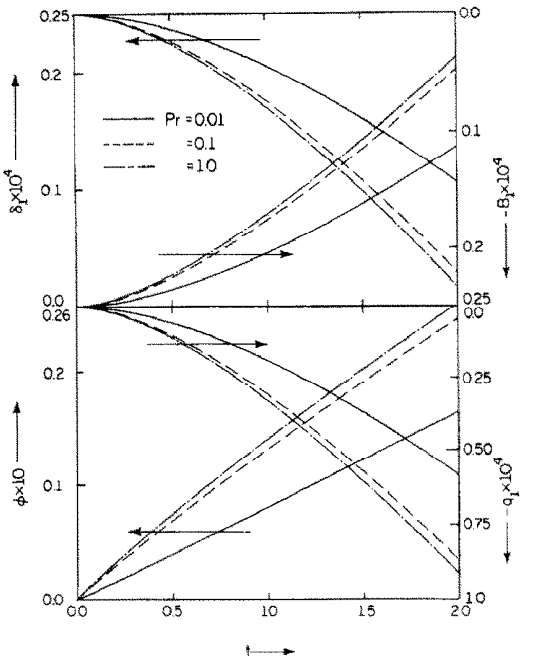

FIG. 6. Prandtl number effects (1st-order solution at $Pr = 1$, $S_b = 1$, $\alpha_{sl} = 1$).

solid is warmed and thus a larger δ_0 at a larger value of α_{sl} results. This also induces more melted solid at a lower value of q_0 as shown in Fig. 5a. The 1st-order solution (free convection) is proportional to the amount of the melted solid. The effects of the free convection increase with α_{sl} as shown in Fig. 5b.

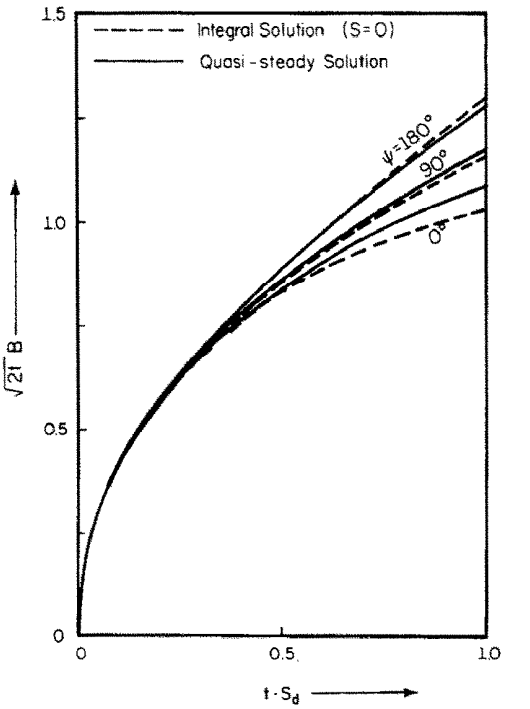

FIG. 7. Comparison of melting front ($Pr = 1$, $S_d = 0.1$, $S_b = 0$, $\alpha_{sl} = 1$).

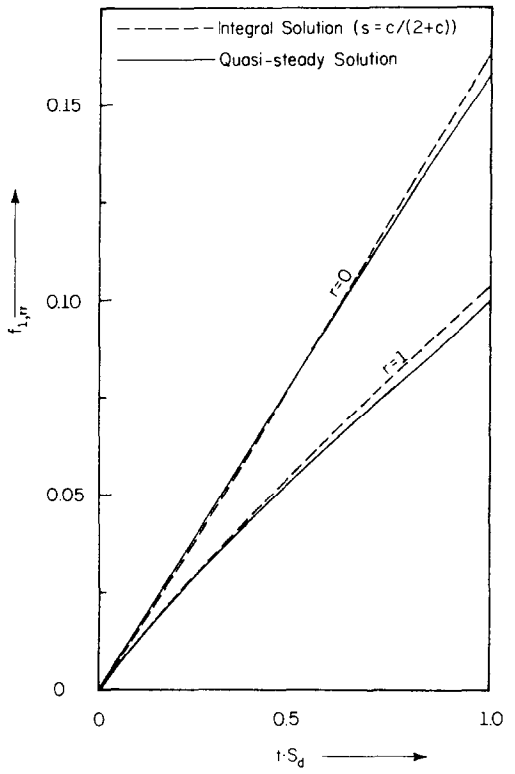

FIG. 8. Comparison of azimuthal shear ($Pr = 1$, $S_d = 0.1$, $S_b = 0$, $\alpha_{sl} = 1$).

Pr only affects the 1st-order solution. Its effect is shown in Fig. 6 for $Pr = 0.01$, 0.1, 1, and 10, respectively. The effects of the free convection are larger at a larger value of Pr. The difference between $Pr = 1$ and 10 is very small; therefore, the data corresponding to $Pr = 10$ are excluded.

The integral solution is compared with the quasi-steady solution in Figs. 7 and 8. In Fig. 8, the locations of melted front are plotted at $\psi = 0°$, 90°, and 180°, respectively; the values of parameters are $Ra = 500$, $Pr = 1$, $\alpha_{sl} = 1$, $S_d = 0.1$, and $S_b = 0$. For $S_d = 0.1$, the quasi-steady solution is expected to be very accurate. Free convection does not affect the melting process at $\psi = 90°$ where the integral solutions agree with the quasi-steady solution within 1%. At $\psi = 0°$, the integral solution predicts a slower melting rate than that of the quasi-steady solution. The difference is bounded by 5% at $S_d(t) = 1$. This indicates that the integral solution predicts a stronger free-convection effect than what the quasi-steady solution predicts.

The assumed stream function, equation (24), with $S = 0$ gives an equal azimuthal shear at $r = 0$ and $r = 1$ which disagrees with the values predicted by the quasi-steady solution. A careful analysis of the quasi-steady solution indicates that the azimuthal shear at $r = 0$ is larger than that at $r = 1$, and their ratio is about $1 + (t/2)^{1/2}(B_0)$. A better comparison of the azimuthal shear is achieved by selecting $S = C/(2 + C)$, shown in Fig. 8. However, it predicts a slightly stronger free convection than that of $S = 0$ (it is about 1% more). The difference of the integral solution at $S = C/(2 + C)$ and the quasi-steady solution is slightly larger than that for $S = 0$. Nevertheless, the accuracy of the integral solution is well within the range of acceptable engineering practice.

REFERENCES

1. E. N. Sparrow, R. R. Schmidt and J. W. Ramsey, Experiments on the role of natural convection in the melting of solids, *J. Heat Transfer* **100**, 11–16 (1978).
2. A. G. Bathlet, R. Viskanta and W. Leidenfrost, An experimental investigation of natural convection in the melted region around a heated horizontal cylinder, *J. Fluid Mech.* **90**(2), 227–239 (1979).
3. L. S. Yao and F. F. Chen, Effects of natural convection in the melted region around a heated horizontal cylinder, *J. Heat Transfer* **102**, 467–474 (1980).
4. E. M. Sparrow, S. V. Patankar and S. Ramadhyani, Analysis of melting in the presence of natural convection in the melted region, *J. Heat Transfer* **99**, 520–526 (1977).
5. E. M. Sparrow, S. Ramadhyani and S. V. Patankar, Effects of subcooling on cylindrical melting, *J. Heat Transfer* **100**, 395–402 (1978).
6. H. S. Carslaw and J. C. Jaeger, *Conduction of Heat in Solids* Oxford University Press, London (1947).

CHANGEMENT DE PHASE VARIABLE AUTOUR D'UN CYLINDRE HORIZONTAL

Résumé—La méthode intégrale est appliquée à l'étude des effets de la convection naturelle sur la fusion d'un solide autour d'un cylindre horizontal chaud. Les résultats montrent que le processus de fusion est lié aux cinq paramètres adimensionnels: le sous-refroidissement, les nombres de Rayleigh, de Stefan, de Prandtl, et le rapport des diffusivités thermiques. Leurs effets sont déterminés quantitativement. La solution intégrale montre une précision surprenante quand on la compare avec la solution quasi-statique pour un nombre de Stefan faible.

INSTATIONÄRER PHASENWECHSEL AN EINEM HORIZONTALEN ZYLINDER

Zusammenfassung—Mit Hilfe der Integral-Methode werden die Einflüsse freier Konvektion auf das Schmelzen eines Feststoffes um einen heißen horizontalen Zylinder untersucht. Die Ergebnisse zeigen, daß der Schmelzvorgang durch die folgenden fünf dimensionslosen Parameter beeinflußt wurd: Unterkühlung Rayleigh-, Stefan- und Prandtl-Zahl und das Verhältnis der Temperaturleit fähigkeiten. Ihre Einflüsse werden quantitativ angegeben. Die integrale Lösung zeigt überraschende Genauigkeit im Vergleich mit der quasi-stationären Lösung bei kleiner Stefan-Zahl.

ПЕРЕХОДНЫЕ ФАЗОВЫЕ ИЗМЕНЕНИЯ У ГОРИЗОНТАЛЬНОГО ЦИЛИНДРА

Аннотация — С помощью интегрального метода исследуется влияние естественной конвекции на плавление твердого вещества вокруг нагретого горизонтального цилиндра. Полученные результаты свидетельствуют о том, что процесс плавления определяется следующими безразмерными параметрами: недогревом, числами Релея, Стефана и Прандтля и отношением коэффициентов температуропроводности. Проведена количественная оценка роли указанных параметров. Интегральное решение дает хорошее совпадение с квазистационарным решением при малых значениях числа Стефана.